

Alkane-Assisted Adsorption and Assembly of Phthalocyanines and Porphyrins

Xiaohui Qiu, Chen Wang, Qingdao Zeng, Bo Xu, Shuxia Yin, Hongna Wang, Shandong Xu, and Chunli Bai*

Contribution from the Center for Molecular Sciences, Institute of Chemistry, Chinese Academy of Sciences, Beijing 100080, China

Received December 6, 1999. Revised Manuscript Received March 9, 2000

Abstract: In this paper it is demonstrated that the stabilizing effect of linear alkanes can be utilized to achieve very high stability in the adsorption and assembly of planar organic molecules on inert surfaces under ambient conditions, by direct deposition from solutions. Using peripherally alkylated phthalocyanines and porphyrins as the examples, optimal resolutions can be achieved with complex molecular systems. Submolecular features of the molecular cores and the interdigitated alkyl parts are clearly visible. Distinctly different packing symmetries were also observed and could be attributed to the intermolecular and adsorbate–substrate interactions. Appreciable contrast variations were also recorded with changing bias voltages. This approach could be adapted to the studies of other molecules to observe submolecular features and could be helpful in obtaining two-dimensional assemblies of monodispersed molecules, especially planar molecules.

1. Introduction

Immobilizing organic molecules on solid surfaces is of considerable interest both toward the goal of high-resolution structural characterizations and for its potential applications. Great efforts have been made toward the goal of immobilizing individual molecules on a substrate, with minimal impact on the chemical and physical properties of the adsorbed molecules. Remarkable progress has been made in the experiments using standard vacuum techniques, for example. These exciting practices have prompted high interest in studying and manipulating individual molecules and further exploring the capability of using STM to identify submolecular structures. The remarkable achievements stimulated illuminating research activities and provided us with a greater understanding of the correlation of electronic structures with the observed STM topography images.

For obtaining stably adsorbed molecules on surfaces, one effective method involves subliming the molecules in ultra-high vacuum (UHV). The unprecedented high resolutions obtained with use of a scanning tunneling microscope (STM), demonstrated in many molecular systems exemplified by phthalocyanines and porphyrins^{1–3} and other aromatic molecules on metal surfaces,⁴ makes it a unique approach for exploring submolecular structures. While UHV environment is ideal for epitaxial growth of molecular films and subsequent studies,⁵ not all species can be adapted to UHV, such as those with relatively low thermal stability. As an alternative approach, the electrochemical method utilizes an electric potential to increase

the affinity of the adsorbates to the conductive substrates.⁶ It was also shown that graphite surfaces can be modified by an acid–base reaction to increase the affinity.⁷ Another method for preparing stable molecular monolayers uses matrix molecules to coadsorb the species of interest, such as liquid crystal (LC) and phthalocyanine molecules on graphite surface⁸ and benzene and CO on Rh⁹ in UHV. However, it has been noticed that, in many cases, the adsorption barrier is not sufficient to keep small molecules on surfaces either in a vacuum or under a solution environment, and the stability of the adsorbed species is a crucial factor in many studies.

In the meantime, pioneering studies using STM have been reported for a number of molecular species with long alkyl tails, such as *n*-alkylcyanobiphenyl (*n*CB).^{10–12} The two-dimensional (2D) lamellae of alkyl chains are considered essential to the stabilization.¹⁰ This important effect of stabilization of organized assemblies by alkyl substituents plays an important role in a series of studies on STM contrast mechanisms of various functional groups (with primary or para-substituted hydrocarbons).^{10–16} It also provides a promising venue for studying a broader range of molecules at the submolecular level, which is worthy of concentrated attention. The effort could help research-

(6) For example, see: Tao, N. J. *Phys. Rev. Lett.* **1996**, *76*, 4066–4069.

(7) Pomerantz, M.; Aviram, A.; McCorkle, R. A.; Li, L.; Schrott, A. G. *Science* **1992**, *255*, 1115–1118.

(8) Freund, J.; Probst, O.; Grafstrom, S.; Dey, S.; Kowalski, J.; Neumann, R.; Wortge, M.; zu Putlitz, G. *J. Vac. Sci. Technol. B* **1994**, *12*, 1914–1917.

(9) Ohtani, H.; Wilson, H. J.; Chiang, S.; Mate, C. M. *Phys. Rev. Lett.* **1988**, *60*, 1418–1421.

(10) (a) Foster, J. S.; Frommer, J. E. *Nature* **1988**, *333*, 542–545. (b) Spong, J. K.; Mizes, H. A.; LaComb, L. J., Jr.; Dovek, M. M.; Frommer, J. E.; Foster, J. S. *Nature* **1989**, *338*, 137–139.

(11) (a) Smith, D. P. E.; Horber, H.; Gerber, Ch.; Binnig, G. *Science* **1989**, *245*, 43–45. (b) Smith, D. P. E.; Horber, J. K. H.; Binnig, G.; Nejjoh, H. *Nature* **1990**, *344*, 641–644.

(12) Walba, D. M.; Stevens, F.; Parks, D. C.; Clark, N. A.; Wand, M. D. *Science* **1995**, *267*, 1144–1147.

(13) (a) Rabe, J. P.; Buchholz, S. *Science* **1991**, *253*, 424–427. (b) Rabe, J. P.; Buchholz, S. *Phys. Rev. Lett.* **1991**, *66*, 2096–2099. (c) Cincotti, S.; Rabe, J. P. *Appl. Phys. Lett.* **1993**, *62*, 3531–3533.

(1) (a) Lippel, P. H.; Wilson, R. J.; Miller, M. D.; Woll, Ch.; Chiang, S. *Phys. Rev. Lett.* **1989**, *62*, 171–174. (b) Chiang, S. *Chem. Rev.* **1997**, *97*, 1083–1096.

(2) (a) Lu, X.; Hipps, K. W.; Wang, X. D.; Mazur, U. *J. Am. Chem. Soc.* **1996**, *118*, 7197–7202. (b) Lu, X.; Hipps, K. W. *J. Phys. Chem. B* **1997**, *101*, 5391–5396.

(3) Jung, T. A.; Schlittler, R. R.; Gimzewski, J. K.; Tang, H.; Joachim, C. *Science* **1996**, *271*, 181–184.

(4) Strohmaier, R.; Petersen, J.; Gompf, B.; Eisenmenger, W. *Surf. Sci.* **1998**, *418*, 91–104.

(5) Forrest, S. R. *Chem. Rev.* **1997**, *97*, 1793–1896.

ers to develop the effect into a more general method to better explore single molecules, as envisioned in the earlier studies.^{10–16}

The interaction between many organic molecules and substrate is generally considered to occur via van der Waals forces in nature, and the magnitude is rather weak. This situation often requires extra effort to achieve satisfactory results in molecular immobilization. On the other hand, attaching molecules to the substrate by chemical bonding would inevitably incur distortions to the molecular structures and properties. It is of interest to use intermolecular force to facilitate the immobilization of molecular species.

Intermolecular forces have been widely recognized in the assembling of molecules. In particular, the adsorption of the assembled alkanes is considered closely related to the intermolecular interactions through 2D crystallization,¹³ in addition to the adsorbate–substrate interactions. This view suggests that close-packed molecules would have a better adsorption stability. Another important factor in studying the adsorbates by using STM is the mobility of the adsorbates within the substrate plane. While many molecules can be readily adsorbed on the substrate surface, their mobility within the basal plane often presents difficulties in obtaining high-resolution results. The scanning tip may also introduce lateral disturbance via mechanical interaction or inhomogeneous distribution of local electric field. The method of lowering temperatures to reduce thermal migrations is effective for some species, while the studies at room temperature and in solution/ambient environments are rather limited. It is also desirable to exploit methods to immobilize molecules in more lenient conditions and on inert surfaces such as graphite. This is of direct relevance to preparing molecular thin films and assemblies.

For planar molecules, such as phthalocyanines and porphyrins—which are also important candidates for molecular electronics devices, even though they are known to lay flat on surfaces—their diffusion barrier is low, and so they could be mobile under the disturbance of the STM tip. Peripherally (tetra-, hexa-, octa-, etc.) attached long-chain alkanes could enhance not only the adsorption stability by increasing the adsorbate–substrate interaction, but also the diffusion barriers in all directions within the basal plane. Studies of alkane-substituted hexabenzocoronene¹⁷ have shown that the substituted species can be satisfactorily adsorbed on the surface of graphite. In addition, for the specific case of phthalocyanines, it was shown that the alkyl substituents do not affect the characteristics (electrical and optical) of phthalocyanines.¹⁸ This result is important to the studies of single chromophores using STM and related methods. As we would illustrate in this work, the methodology of using substituted alkanes to immobilize single molecules could be applied to achieve rather high resolutions on phthalocyanines and porphyrins under ambient conditions, comparable to those

obtained under UHV conditions. This would enable further investigations of a variety of organic species.

Herein we present the results of using covalently bonded alkanes to assist in the adsorption of planar molecules, taking octa-substituted copper phthalocyanines and tetra-substituted porphyrins as examples. The submolecular features of copper phthalocyanines and porphyrins, together with interdigitated alkanes, were well resolved at different tunneling conditions. The results would allow further investigations of the possible effects of electronic orbitals of adsorbate molecules on the observed STM images. Different packing symmetries were also observed, which could be attributed to the combination of intermolecular and molecule–substrate forces.

2. Materials and Methods

Copper Phthalocyanine. Copper(II) octaalkoxyl-substituted phthalocyanine (purity > 95%, Aldrich Inc.), denoted as CuPcOC8, was obtained from Aldrich and used without further purification. CuPcOC8 has transition temperatures of 112 °C from the crystalline to the discotic mesophase and 85 °C from the discotic to the crystalline phase.¹⁹

Synthesis of TTPP. 21,23-Dihydro-5,10,15,20-tetrakis(4-(tetradecyloxy)phenyl)porphyrin (hereafter referred to as TTPP; the molecular structure is shown in Figure 6a later in the text). Details of the synthesis and characterization data are given in the following and in the Supporting Information. The ¹H NMR spectrum was recorded in CDCl₃ on a Varian Unity 200-MHz spectrometer with tetramethylsilane (TMS) as external standard. The MALDI-TOF mass spectrum was recorded on a BIFLEX III (Bruker Inc.). The IR measurement was performed with a Perkin-Elmer 782 spectrometer. Elemental analysis was carried out by the Analytical Laboratory of the Institute of Chemistry, Chinese Academy of Sciences.

Freshly distilled pyrrole (2 g, 29 mmol) was slowly added under stirring to a solution of 4-(tetradecyloxy)benzaldehyde (ref 20) (9.2 g, 29 mmol) in 150 mL of refluxing propionic acid. Refluxing was continued for 3 h, after which the propionic acid was removed under vacuum. The porphyrin was isolated by column chromatography (silica, eluent CHCl₃/MeOH, 9/1, v/v) as a purple powder, yield 1.2 g (11%). ¹H NMR (CDCl₃): δ 8.86 (s, 8H, β-pyrrole), 8.13 (d, 8H, 2,6-phenyl), 7.39 (d, 8H, 3,5-phenyl), 4.26 (t, 8H, OCH₂), 1.2–1.8 (b, 96H, CH₂), 0.9 (t, 12H, CH₃), –2.76 (b, 2H, NH). MALDI-TOF MS (matrix, α-cyano-4-hydroxycinnamic acid): *m/z* = 1464 (M). IR (neat): *ν*/cm^{–1} 1608 (C=C), 1510 (C=C), 1176 (C–O), 804 (C–H). Anal. Calcd for C₁₀₀H₁₄₂N₄O₄: C, 82.03; H, 9.78; N, 3.83. Found: C, 81.83; H, 9.84; N, 3.88.

Methods. The samples were dissolved in phenyloctane (HPLC grade, Aldrich Inc.) or toluene (HPLC grade, Aldrich Inc.) with a concentration of less than 1%. A droplet of the solution was deposited onto a freshly cleaved surface of HOPG. The substrate was incubated at 60 °C for about 5 min and cooled slowly to room temperature. This treatment is employed as a precautionary measure to prepare uniform molecular layers, considering the above-mentioned transition temperatures. In our subsequent experiments, we also obtained very high quality results with the samples that did not undergo heat treatment. Therefore, the incubation procedure should not be a strict protocol, and we would like to leave it as an optional preparation step.

The experiments were performed on Nanoscope IIIa SPM (Digital Instruments, Santa Barbara, CA) under ambient conditions. The STM tips were mechanically formed PtIr wire (90/10).

Preliminary simulations were performed using the Hyperchem software package to model the structure of the copper phthalocyanines and porphyrins. The stable configuration and the electron density of the molecular orbitals were obtained by semiempirical quantum mechanics method of ZINDO/1. Molecular mechanics simulations were performed using the Insight II software package with an SGI workstation.

(19) van der Pol, J. F.; Neeleman, E.; Zwikker, J. W.; Nolte, R. J. M.; Drenth, W.; Aerts, J.; Visser, R.; Picken, S. J. *Liq. Cryst.* **1989**, *6*, 577–592.

(20) Gray, G. W.; Jones, B. *J. Chem. Soc.* **1954**, 1467–1470.

(14) (a) Claypool, C. L.; Faglioni, F.; Goddard, W. A., III; Gray, H. B.; Lewis, N. S.; Marcus, R. A. *J. Phys. Chem. B* **1997**, *101*, 5978–5995. (b) Faglioni, F.; Claypool, C. L.; Lewis, N. S.; Goddard, W. A., III. *J. Phys. Chem. B* **1997**, *101*, 5996–6020. (c) Claypool, C. L.; Faglioni, F.; Goddard, W. A., III; Lewis, N. S. *J. Phys. Chem. B* **1999**, *103*, 7077–7080.

(15) (a) Cyr, D. M.; Venkataraman, B.; Flynn, G. W.; Black, A.; Whitesides, G. M. *J. Phys. Chem. B* **1996**, *100*, 13747–13759. (b) Giancarlo, L. C.; Fang, H.; Rubin, S. M.; Bront, A. A.; Flynn, G. W. *J. Phys. Chem. B* **1998**, *102*, 10255–10263. (c) Giancarlo, L.; Cyr, D.; Muyskens, K.; Flynn, G. W. *Langmuir* **1998**, *14*, 1465–1471.

(16) Lee, H. S.; Iyengar, S.; Musselman, I. H. *Langmuir* **1998**, *14*, 7475–7483.

(17) (a) Stabel, A.; Herwig, P.; Mullen, K.; Rabe, J. P. *Angew. Chem., Int. Ed. Engl.* **1995**, *34*, 1609–1611. (b) Rabe, J. P.; Buchholz, S.; Askadskaya, L. *Synth. Met.* **1993**, *54*, 339–349.

(18) Sauer, T.; Wegner, G. *Mol. Cryst. Liq. Cryst.* **1988**, *162B*, 97–118.

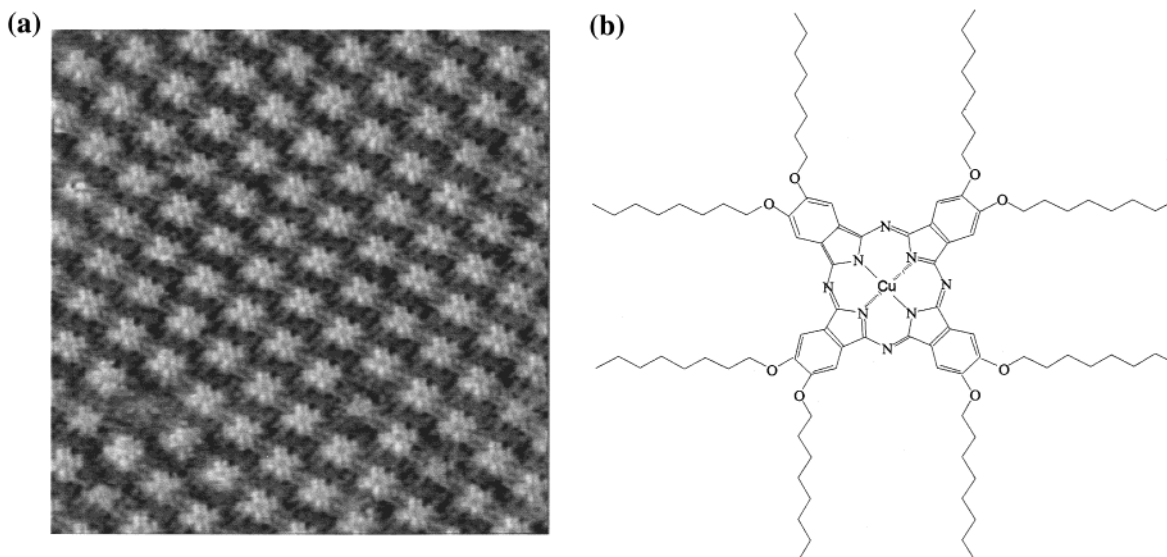


Figure 1. (a) STM image of a self-assembled monolayer of CuPcOC8 on a graphite surface in phenyloctane solvent. Tunneling conditions: 398 pA, -648 mV (sample and hereafter); scan area, 25.2 nm \times 25.2 nm. (b) Molecular structure of CuPcOC8.

3. Results and Discussions

As typical colorant materials, phthalocyanines and porphyrins have been widely studied by various techniques, including STM. Alkane-substituted (alkyl, alkoxyethyl, or branched alkoxy hydrocarbon chains, etc.) phthalocyanines and porphyrins form a typical category of discotic liquid crystals. Both IR and electronic spectra reveal that the substituted phthalocyanines at low concentrations are the same as the phthalocyanine chromophore, while the features of the substituents could also be clearly identified.^{18,21} For alkyl-substituted phthalocyanines, X-ray data show a hexagonal pattern in the discotic mesophase, with the side-chain segments homogeneously distributed in the space between columns.²¹

Observations using STM reveal that the as-prepared CuPcOC8 samples form large, uniform regions of molecular arrays with sizes ranging from tens to hundreds of nanometers, as shown in Figure 1a, with the corresponding molecular structure shown in Figure 1b. It can be seen that the phthalocyanine molecules (appearing as bright spots with four-fold symmetry) form ordered two-dimensional arrays. The shaded zigzag lines interconnecting the bright regions correspond to the long alkyl substituents. The observation clearly indicates that the contributions from phthalocyanine molecules dominate the overall contrast, as expected from theoretical calculations. Detailed examination of the STM image reveals that the alkyl chains of the adjacent molecules interdigitate, as expected for the crystalline phase. The distances between the centers of the neighboring bright spots (positions of phthalocyanine cores) in the two arrangements (explained in the following text) are nearly equal, ~ 2.6 nm, to the peak-to-peak distance. Through adjustment of the length of the attached alkane chains, one might be able to tailor the intermolecular spacing.

Two typical kinds of packing arrangement, quadratic and hexagonal symmetries, were observed to coexist in the monolayer. Figure 2a presents adjacent parallel domains with rather different symmetries. The left domain has a nearly close-packing symmetry, while that in the center and at the right have a typical

four-fold symmetry. For the domains with nearly four-fold symmetry, one could count 16 interdigitated chains in the moieties at the immediate vicinity of a phthalocyanine core, which could be attributed to the aliphatic parts. However, for the hexagonal domains or the appreciably distorted regions, it may be difficult to determine precisely the numbers of alkane chains in the moieties from the STM image. This could be due to the fact that the packaging of the molecules in such symmetries may cause local disorder of the aliphatic parts, as will be discussed later. Although single molecular defects were sometimes observed in the monolayer, the formed two-dimensional network could be reproducibly observed in large areas, indicating a high stability of the self-assembled configurations. The existence of the polymorphs was observable in both phenyloctane and toluene solvents, as described previously.

Figure 2b illustrates the proposed molecular arrangement according to molecular mechanics simulation, as a schematic illustration of the four-fold domain structures. The assembly structure is mainly associated with the intermolecular interactions. The nearly quadratic arrangement is also reported for phthalocyanine molecules formed on graphite, MoS₂, and ionic crystal surfaces with the MBE method.^{5,22} It is well known that the film growth of large organic molecules is determined by the molecule–molecule and molecule–substrate interactions.⁵ In general, a weak molecule–substrate interaction would lead to epitaxial growth of the molecular film, with less distortions of symmetry from its bulk structures, as in the case for copper phthalocyanines on graphite and MoS₂.²² For strong molecule–substrate interactions, the substrate will have a significant impact on the symmetry of the molecular overlayer, causing distortions of the molecular lattice to achieve optimal alignment or commensurability with the substrate lattice, similar to the situation for the epitaxial growth of copper phthalocyanines on a number of semiconductor surfaces.^{5,23} The observed coexistence of the polymorphs in this study is direct evidence of the respective effects of the molecule–molecule and molecule–substrate interactions. The four-fold symmetry is an indication

(21) (a) Piechocki, C.; Simon, J.; Skoulios, A.; Guillon, D.; Weber, P. *J. Am. Chem. Soc.* **1982**, *104*, 5245–5247. (b) Guillon, D.; Skoulios, A.; Piechocki, C.; Simon, J.; Weker, P. *Mol. Cryst. Liq. Cryst.* **1983**, *100*, 275–284. (c) Guillon, D.; Weber, P.; Skoulios, A.; Piechocki, C.; Simon, J. *Mol. Cryst. Liq. Cryst.* **1985**, *130*, 223–229.

(22) Ludwig, C.; Strohmaier, R.; Petersen, J.; Gompf, B.; Eisenmenger, W. *J. Vac. Sci. Technol. B* **1994**, *12*, 1963–1966. Collins, G. E.; Nebesny, K. W.; England, C. D.; Chau, L.-K.; Lee, P. A.; Parkinson, B. A.; Armstrong, N. R. *J. Vac. Sci. Technol. A* **1992**, *10*, 2902–2913.

(23) Cox, J. J.; Bayliss, S. M.; Jones, T. S. *Surf. Sci.* **1999**, *425*, 326–333.

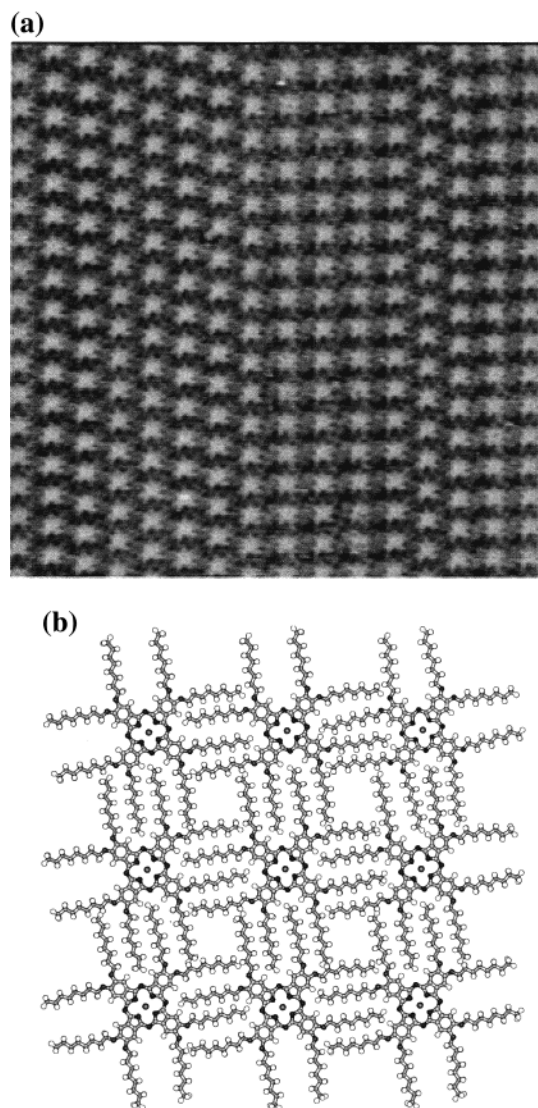


Figure 2. (a) STM image showing the coexistence of the domains with different symmetries. Tunneling conditions: 909 pA, -742 mV; scan area, 43.0 nm \times 43.0 nm. (b) Molecular mechanics simulation of quadratic arrangement of CuPcOC8 as deduced from STM images.

of relatively weak molecule–substrate interactions. On the other hand, the molecule–substrate interaction (as will be discussed later) is partly due to the electrostatic interaction of the copper atom with the substrate (which could be more significant on ionic crystal surfaces⁵) and is considerably enhanced by the long alkane chains bonded to phthalocyanines. Considering that it has been well established that alkanes will align with the substrate registry in their stabilized assemblies, the observed six-fold symmetry in this study is not surprising. In addition, as the result of the compromise of the strengths of the above-mentioned interactions, intermediate symmetries, such as nearly hexagonal or nearly quadratic arrangements, also arise as observed in the presented figures. Further experiments on the polymorphic phenomena would be helpful by allowing comparison of the molecular lattices from different systems with various ligand metal atoms and substituent lengths.

Figure 3a,b shows high-resolution STM images of CuPcOC8 at positive and negative sample bias, respectively. For the images at negative sample bias, the submolecular structure of individual molecules (Figure 3a) can be clearly resolved. Figure 3a is an image of the molecules in a nearly six-fold symmetry region. The equivalent resolutions of the molecules at different orienta-

tions indicate that the tip is reasonably symmetric. The images recorded in both four-fold and six-fold symmetries are nearly identical, in that the inner ring is formed by eight symmetrical bright spots, which are attributed to the conjugated phthalocyanine ring. The surrounding lobelike regions are associated with the phenyl groups of the phthalocyanine. The side width of the central bright regions (including the phenyl groups) is 1.65 ± 0.05 nm, which is consistent with the reported side width of 1.70 nm estimated for the octahydroxyphthalocyanine core.²⁴

Submolecular features can also be observed at positive sample bias, as shown in Figure 3b. The fine features indicate the presence of protrusions in the central region, which is different from the features recorded at negative sample bias.

The calculation of the electronic structure of copper phthalocyanine agrees very well with the D_{4h} symmetry of the molecular structure determined from X-ray diffraction data. Figure 4a–d illustrates the charge density contours of the HOMO and LUMO of the copper phthalocyanine core, calculated by ZINDO/1. Figure 4a,b presents the charge densities associated with the HOMO and LUMO respectively, with the contour plots at 1 Å away from the molecular plane given in Figure 4c,d. The charge density of the HOMO has an inner ring with eight maximum points arranged in four-fold symmetry in association with the indole ring. One can observe that the indole ring is the dominant contributing factor. There are four additional small lobes of charge density attached to the phthalocyanine ring. Copper appears as a weak maximum at the center (Figure 4b) and decays off quickly, moving away from the molecular plane (Figure 4d). These calculations are helpful in analyzing the fine features and the dimensions of the observed molecules.

It is worth pointing out that, even though a certain resemblance between the calculated charge density distributions for the observed STM images can be observed, a direct relationship may still deserve extensive study. There are several factors that should be seriously considered in the theoretical analysis. The coupling of the wave functions, or tunneling matrix, between the tip and the surface (adsorbate and substrate) at various tip–sample separations could be quite different, since the charge density contours of the molecules are sensitive to the distance from the central molecular plane. This can be seen from the contour plots for charge densities at different distances from the molecular plane (e.g., Figure 4b,d). The substrate electronic structures could influence the STM contrast. For example, it is reported that the contrast for long-chain hydrocarbons displays certain variations on different substrates.^{15b} Another important factor is the commensurability of the molecular lattice with the substrate lattice, which may lead to different coupling between the tip and surface wave functions. Therefore, the effects associated with the observed different symmetries may not be neglected. However, a full-fledged analysis of the observed submolecular features should include more systematic experimental, and particularly theoretical, investigations taking into account the effects of intrinsic molecular electric front orbital, tip, and substrate properties, as shown in many previous studies.^{14b}

As just described, high-resolution STM images of the CuPcOC8 molecules can be obtained over a wide range of bias voltage and both bias voltage polarities. While the higher voltage produces a stronger image contrast between the phthalocyanine cores and the alkyl substituents, lowering the voltage leads the alkyl chains to become more pronounced. Upon further lowering

(24) Schouten, P. G.; Warman, J. M.; Gelinck, Copyn, M. J. *J. Phys. Chem.* **1995**, *99*, 11780–11793.

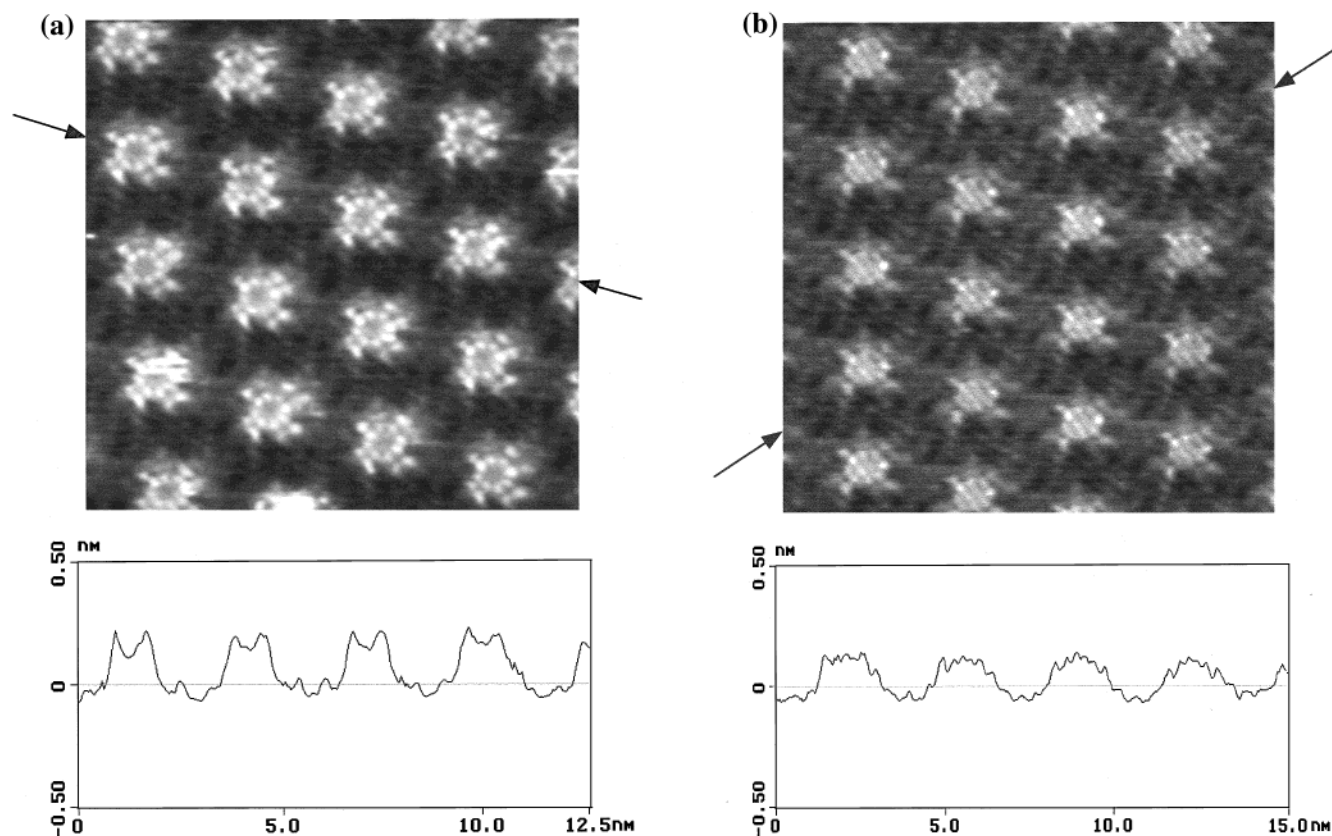


Figure 3. High-resolution STM images of CuPcOC8 at both polarities. (a) Tunneling conditions: 909 pA, -582 mV; scan area, 12.8 nm \times 12.8 nm. (b) Image of CuPcOC8 at positive sample bias. Imaging conditions: 909 pA, 742 mV; scan area, 13.3 nm \times 13.3 nm.

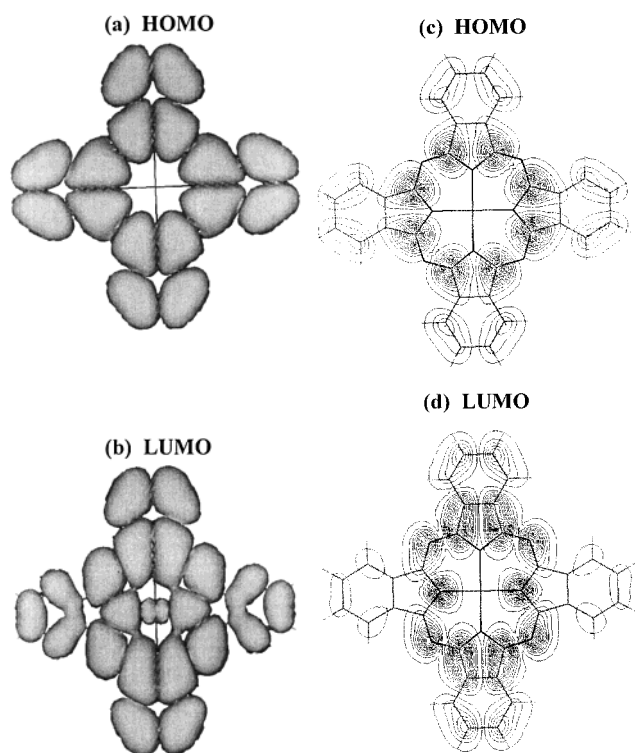


Figure 4. Charge density distributions of copper phthalocyanine, (a) HOMO and (b) LUMO, and the contour plots of the charge densities 1 Å from the molecular plane, (c) HOMO and (d) LUMO.

the bias voltage (typically less than 100 mV, depending on the tip), the underlying graphite substrate becomes visible. This practice would enable us to verify the calibration of the scanner

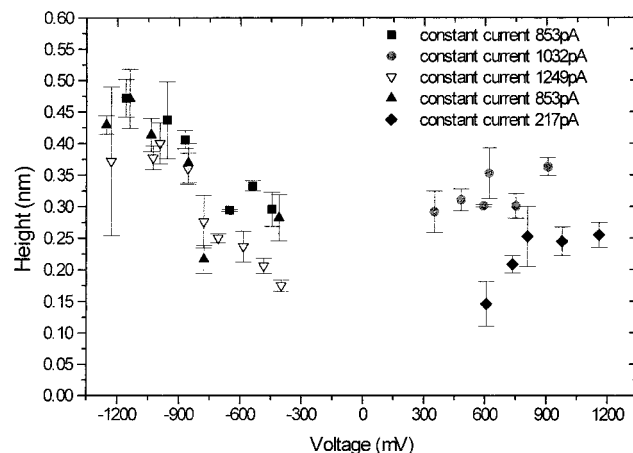


Figure 5. Measured height of copper phthalocyanines versus applied bias voltage.

head during operation to ensure reliable measurements of the dimensions of the adsorbed molecules.

By measuring the relative height at the single molecular defects or exposed graphite substrate surface, it is possible to identify the height as about 0.2–0.4 nm for CuPcOC8. Figure 5 gives the heights measured versus tunneling bias voltage of CuPcOC8 while the tunneling current was kept constant. Since the alkanes do not show appreciable contrast variations versus bias voltage, the moieties of aliphatic parts between the phthalocyanine cores could also be used as a reasonable reference to measure the contrast variations of the phthalocyanine cores. The measured heights are consistent with the previously reported data¹ and also indicate that the phthalocyanine molecules are adsorbed with their molecular plane parallel to the graphite substrate.

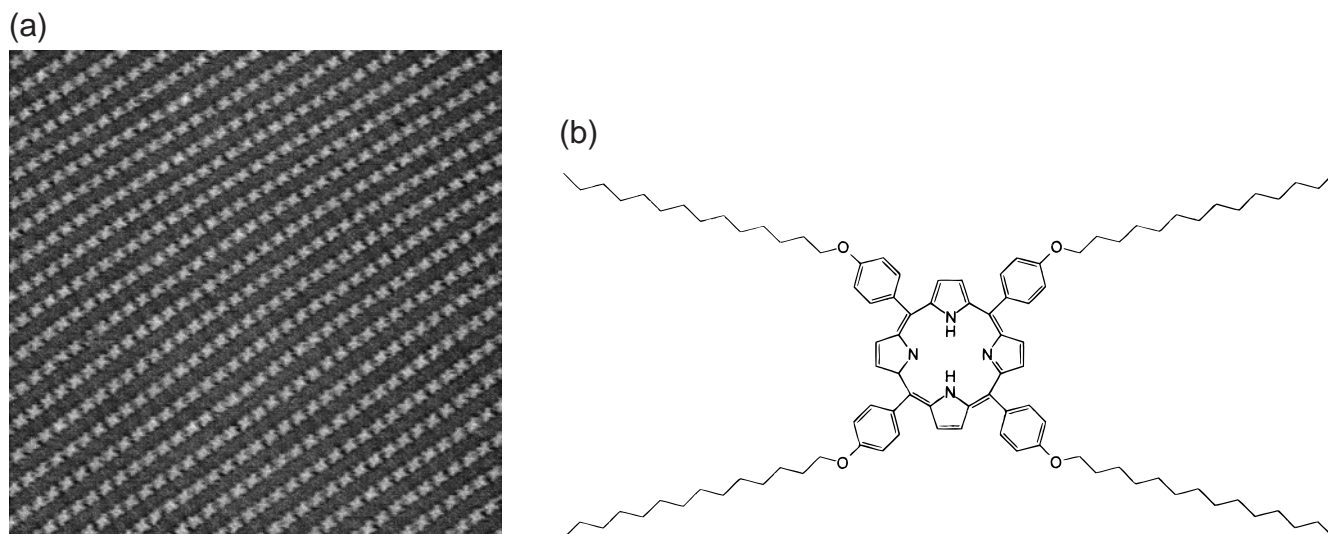


Figure 6. STM observation of TTPP. (a) Large, uniform domains with rows of porphyrin lines separated by alkane lamellae. Tunneling conditions: 680 mV, 1.12 nA; scan area, 67.5 nm \times 67.5 nm. (b) Molecular structure of TTPP.

In comparison to typical deposition methods, where the adsorption or immobilization is due to the electrostatic interaction of oppositely charged molecules and surfaces, the adsorption of molecules in this work is presumably dominated by the assembling nature of the molecules and van der Waals forces, as mentioned in the Introduction. Here, we would estimate the adsorption barrier from the adsorbate–substrate interaction. According to calculations by Hentschke et al.,²⁵ each $-\text{CH}_2$ of the alkyl chain on graphite will provide as much as 70 meV adsorption potential for fully commensurate registry. Accordingly, the total adsorption energy associated with the eight octyl chains in CuPcOC8 could amount to more than 4 eV.²⁶ It is obvious that the total desorption barrier of a combined molecule is significantly higher than that of a single phthalocyanine molecule. Therefore, the adsorption stability of the alkylated phthalocyanine molecules could be greatly improved, and the scheme could be used to study other organic molecules at liquid/solid or air/solid interfaces. Furthermore, the closely assembled alkane chains surrounding phthalocyanine cores will substantially enhance the adsorption stability, as well as the diffusion barrier, in all directions within the basal plane. This helps to explain the effect of the attached aliphatic chains on immobilizing the chromophores within the substrate basal plane.

Similar studies could be expanded to other molecular systems, such as derivatives of phthalocyanines and porphyrins with alkyl substituents, etc. Figure 6a shows the STM observation of tetra-substituted porphyrin TTPP, with the molecular structure given in Figure 6b. The large, uniform domains indicate high stability of the assembly. Observations were carried out over a range of bias values at both positive and negative sample biases. The examples are given in Figure 7a,b. The figures show that porphyrins are aligned side-by-side, separated by the alkane lamellae, which is a direct indication of the effect of 2D crystallization of alkanes. This result indicates that the assembly formation is directly affected by the coordination of the alkane substituents, as first revealed in the assembly of alkane-substituted hexabenzocoronene.¹⁷ Since the alkanes are grouped in the lamellae, adjusting the alkane chain length could only vary the spacing between porphyrin rows, different from

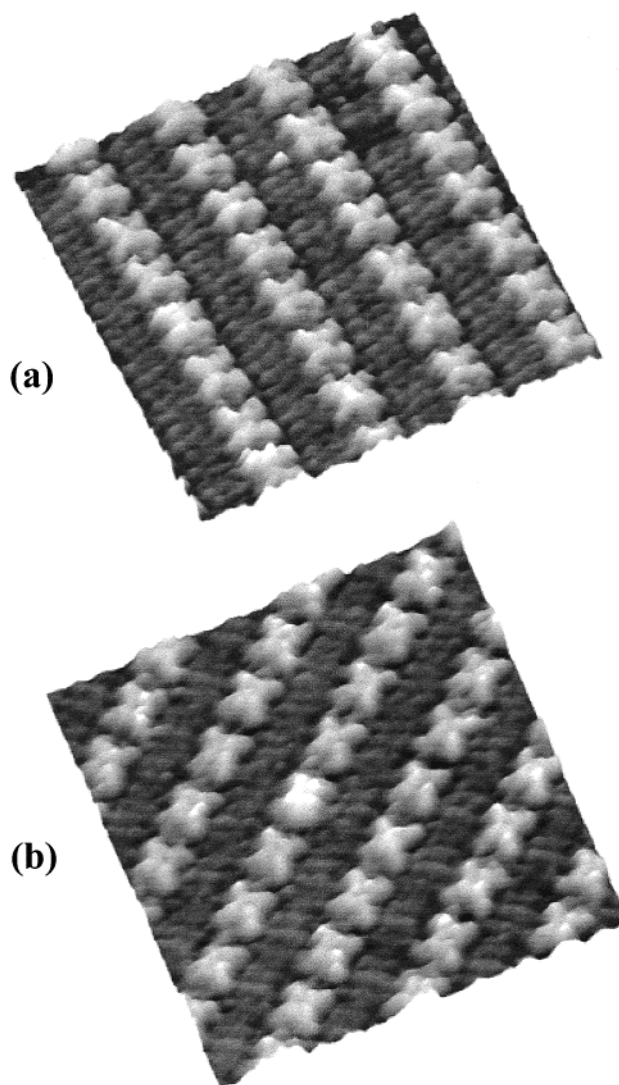


Figure 7. High-magnification STM images of TTPP. (a) Tunneling conditions: 817 mV, 1.06 nA; scan area, 15.2 nm \times 15.2 nm. (b) Tunneling conditions: -680 mV, 1.12 nA; scan area, 15.1 nm \times 15.1 nm.

(25) Hentschke, R.; Schurmann, B. L.; Rabe, J. P. *J. Chem. Phys.* **1992**, *96*, 6213–6221.

(26) Qiu, X. H.; Wang, C.; Yin, S. X.; Zeng, Q. D.; Xu, B.; Bai, C. L. *J. Phys. Chem. B* **2000**, *104*, 3570–3574.

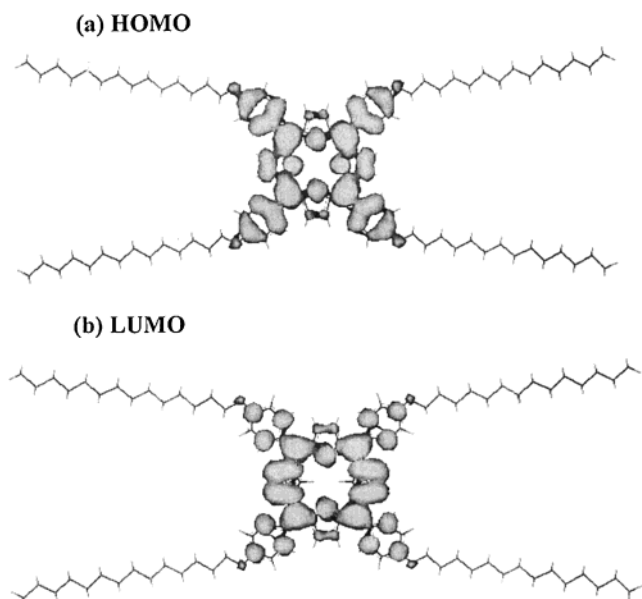


Figure 8. Charge density distributions of TTPP: (a) HOMO and (b) LUMO.

adjusting the nearest-neighbor spacing in the case CuPcOC8. The results also suggest that the method discussed in this work could complement other studies on porphyrins under UHV³ and electrochemical conditions.⁶

Parallel to the discussions on CuPcOC8, Figure 8 shows the calculated electrical orbitals of TTPP and can be compared with the observed STM images. The coordinations of the four-lobe feature in the molecule core coincide with the calculated results. It is also worth mentioning that, while the electrical orbital might play an important role in the observed features at molecular cores, the observation of alkanes would be associated with other models taking into account both topography and electrical structures.¹⁴ It again stresses the need for more systematic theoretical investigations.

It should be noted that the previously reported observations, together with this study, once again illustrate that properly designed and coordinated molecules could better utilize the high-resolution capability of STM at the single-molecule level, in general conditions such as organic solutions and ambient. One could also introduce various substituent symmetries, end groups, etc. to form different types of molecular assemblies. This would also allow the study of a variety of monodispersed individual molecules, with adjustable separations between core molecules,

by spectroscopic methods in association with STM. Further studies are deemed necessary in relation to the substituent length effects and core molecule affinity effects, which will lead to better control of the molecular assemblies established at solvent/solid and air/solid interfaces.

For the molecular systems studied in this work, it is known that phthalocyanines and porphyrins (together with their various substituted derivatives) could form columns of stacked phthalocyanines to produce molecular wires, either by simple stacking of the chromophores or by ionic bridging (ligand connections).²¹ The alkanes have shown appreciable effects in separating the columns. One may therefore also use the surface-bound assemblies as a template to grow one-dimensional molecular wires perpendicular to the basal plane, which could have potential applications.

4. Summary

The observations presented in this work demonstrate that by using substituted long-chains alkanes as molecular anchors or immobilizers, the phthalocyanines and porphyrins can be ultimately immobilized at substrate surfaces to allow high-resolution STM studies, which are comparable with those obtained under ultra-high-vacuum conditions. The resulting high stability and close-packed assembly are attributed to the increased adsorption barrier in association with alkanes. The observations illustrate an improvement of the previously reported sample preparation practices that will allow studies to be done under more general conditions, which could complement the ultra-high-vacuum conditions, and can be adapted to the studies of other organic molecules. The observed existence of polymorphs revealed the joint effects of intermolecular and molecule-substrate interactions. This method could also allow researchers to obtain two-dimensional assemblies of monodispersed molecules on inert surfaces.

Acknowledgment. The authors thank the National Natural Science Foundation and the Foundation of the Chinese Academy of Sciences for financial support. They also thank Prof. Li Lemin for helpful discussions on semiepirical calculations of the molecular orbitals.

Supporting Information Available: ¹H NMR spectrum, MALDI-TOF mass spectrum, and IR measurements of the compound TTPP (PDF). This material is available free of charge via the Internet at <http://pubs.acs.org>.

JA994271P